WRINKLED1 Regulates BIOTIN ATTACHMENT DOMAIN-CONTAINING Proteins that Inhibit Fatty Acid Synthesis[1][OPEN]

Hui Liu,[2] Zhiyang Zhai,[2] Kate Kuczynski, Jantana Keereetaweep, Jorg Schwender, and John Shanklin[3,4]

Department of Biology, Brookhaven National Laboratory 463, Upton, New York 11973

ORCID IDs: 0000-0001-8524-1759 (H.L.); 0000-0003-3181-1773 (Z.Z.); 0000-0002-0625-1017 (K.K.); 0000-0001-8314-9289 (J.K.); 0000-0003-1350-4171 (J.Sc.); 0000-0002-6774-8043 (J.Sh.).

WRINKLED1 (WRI1) is a transcriptional activator that binds to a conserved sequence (designated as AW box) boxes in the promoters of many genes from central metabolism and fatty acid (FA) synthesis, resulting in their transcription. BIOTIN ATTACHMENT DOMAIN-CONTAINING (BADC) proteins lack a biotin-attachment domain and are therefore inactive, but in the presence of excess FA, BADC1 and BADC3 are primarily responsible for the observed long-term irreversible inhibition of ACETYL-COA CARBOXYLASE, and consequently FA synthesis. Here, we tested the interaction of WRI1 with *BADC* genes in Arabidopsis (*Arabidopsis thaliana*) and found purified WRI1 bound with high affinity to canonical AW boxes from the promoters of all three *BADC* genes. Consistent with this observation, both expression of *BADC1*, *BADC2*, and *BADC3* genes and BADC1 protein levels were reduced in *wri1-1* relative to the wild type, and elevated upon *WRI1* overexpression. The double mutant *badc1 badc2* phenocopied *wri1-1* with respect to both reduction in root length and elevation of indole-3-acetic acid-Asp levels relative to the wild type. Overexpression of *BADC1* in *wri1-1* decreased indole-3-acetic acid-Asp content and partially rescued its short-root phenotype, demonstrating a role for BADCs in seedling establishment. That WRI1 positively regulates genes encoding both FA synthesis and BADC proteins (i.e. conditional inhibitors of FA synthesis), represents a coordinated mechanism to achieve lipid homeostasis in which plants couple the transcription of their FA synthetic capacity with their capacity to biochemically downregulate it.

Lipids are primary metabolites in cells, acting as structural components of cell membranes, energy-dense storage compounds, and cell signaling molecules. Fatty acids (FAs) are major components of lipids and triacylglycerols (TAGs), which are storage lipids that accumulate mostly in oil bodies in plant seeds (Li-Beisson et al., 2013). De novo synthesis of FAs occurs in the plastid via a well-established pathway (Ohlrogge and Browse, 1995; Rawsthorne, 2002), In Arabidopsis (*Arabidopsis thaliana*), transcription factors (TFs) LEAFY COTYLEDON1 (LEC1) and LEC2, FUSCA3, and ABSCISIC ACID INSENSITIVE3 serve as the master regulators of embryogenesis and seed maturation (Parcy et al., 1997; Lotan et al., 1998; To et al., 2006) and also regulate accumulation of TAG (Kagaya et al., 2005; Santos Mendoza et al., 2005; Braybrook et al., 2006). WRINKLED1 (WRI1), an APETALA2-type TF, functions downstream of LEC1 and LEC2 (Baud et al., 2007; Mu et al., 2008) and is a master regulator of FA synthesis (FAS) because seeds of the WRI1 mutant show an 80% reduction in TAGs compared to the wild type (Focks and Benning, 1998). More than 20 *WRI1* target genes have been identified by comparing gene expression in the wild type with that of *wri1* and *WRI1* overexpression-lines, and electrophoretic mobility shift assays confirmed WRI1-gene promoter binding. Based on promoter sequence comparisons, [CnTnG](n)$_7$[CG] was identified as the consensus WRI1 binding site (designated as AW box). WRI1 target sequences are found upstream of genes coding for enzymes involved in glycolysis (Suc synthase, pyruvate kinase, and pyruvate dehydrogenase), Glu-6P and phospho*enol*pyruvate plastidial transporters (Glu-6P/phosphate translocator and phospho*enol*pyruvate/phosphate translocator), subunits of acetyl-CoA carboxylase (ACCase; biotin carboxyl carrier protein 2 [BCCP2], biotin carboxylase, and carboxyltransferase), FAS (malonyl-CoA:acyl carrier

[1]This work was supported by grants from the Division of Chemical Sciences, Geosciences, and Biosciences, Office of Basic Energy Sciences, U.S. Department of Energy (DOE KC0304000 to J.Sh. and DE-SC0012704 to J.Sc.) and by a National Science Foundation grant under which initial discussions took place and several reagents were made (DBI 1117680 to J.Sh. and J.Sc.).

[2]These authors contributed equally to this article.

[3]Author for contact: shanklin@bnl.gov.

[4]Senior author.

The author responsible for distribution of materials integral to the findings presented in this article in accordance with the policy described in the Instructions for Authors (www.plantphysiol.org) is: John Shanklin (shanklin@bnl.gov).

H.L, Z.Z. J.Sc., J.K., and J.Sh. conceived the original research plans and designed the experiments; H.L, K.K., Z.Z., and J.K. performed the experiments; and H.L, Z.Z. J.Sc., J.K., and J.Sh. analyzed the data and wrote the article with contributions from all the authors.

[OPEN]Articles can be viewed without a subscription.

www.plantphysiol.org/cgi/doi/10.1104/pp.19.00587

protein [ACP] malonytransferase, ketoacyl-ACP synthase, hydroxyacyl-ACP dehydrase, enoyl-ACP reductase, ACPs, and oleoyl-ACP thioesterase), and genes involved in synthesis of lipoic acid, a cofactor of pyruvate dehydrogenase (Ruuska et al., 2002; Baud et al., 2007; Maeo et al., 2009; Fukuda et al., 2013; Li et al., 2015). Interestingly, genes involved in TAG synthesis and oil body assembly, such as diacylglycerol acyltransferase 1, which catalyzes the final step of TAG synthesis, and oleosins and caleosins appear not to be regulated by WRI1, though some species-specific variation has been reported (Maeo et al., 2009; Grimberg et al., 2015). Characterizing gene expression of subunits of ACCase revealed that the distance between the AW site and the translational initiation site (TIS) strongly influences the function of the AW box (Fukuda et al., 2013) in that the majority of AW sites fall within 200 bp of the TIS in genuine WRI1 target genes (Maeo et al., 2009; Fukuda et al., 2013).

A class of proteins annotated as biotin attachment domain containing (BADC; Olinares et al., 2010) have been recently identified as inhibitors of FAS (Salie et al., 2016; Keereetaweep et al., 2018). BADC proteins are homologs of BCCP, sharing 25% to 30% sequence similarity, but they lack a biotin attachment site, rendering them inactive. All three Arabidopsis BADC isoforms interact with BCCP. Displacement of functional BCCP subunits in ACCase by inactive BADC subunits is believed to reduce the ACCase catalytic activity (Salie et al., 2016). ACCase is subject to feedback regulation upon exposure to exogenously supplied FAs in the form of Tween esters (Tween-80 containing predominantly oleic acid [18:1]). Short-term exposure results in reversible inhibition of ACCase, whereas longer-term exposure results in irreversible inhibition (Andre et al., 2012). Oleoyl-ACP mediates the reversible phase of inhibition (Andre et al., 2012), whereas BADC1 and BADC3 are primarily responsible for the phase of irreversible inhibition (Keereetaweep et al., 2018).

In this work we present evidence that the expression of all three *BADC* genes is under the control of the WRI1 TF. The short-root phenotype and elevated conjugated indole-3-acetic acid (IAA) levels common to the *wri1-1* and the *badc1 badc2* double mutant led us to hypothesize that BADC deficiency is responsible for the observed short-root phenotype. Restoration of near-wild type root length upon overexpression of BADC1 in both *wri1* and *badc1 badc2* is consistent with a yet-to-be identified role for BADCs in seedling development.

RESULTS

The *badc1 badc2* Double Mutant Shows Reduced Primary Root Growth and Fewer Lateral Roots Compared to the Wild Type

Seeds of the *badc1 badc2* double mutant generated in our previous study contained 17% and 23% increases in total FA and TAG accumulation, respectively, compared to the wild type (Keereetaweep et al., 2018). When grown on vertical Murashige and Skoog (MS) plates, *badc1 badc2* exhibited a 62% reduction in primary root length and a 39% decrease in lateral root number compared with the wild type (Fig. 1, A–C). In contrast, root growth of *badc1* or *badc2* single mutants showed no differences from that of the wild type. A complementation experiment was performed in which either *BADC1* or *BADC2* was expressed under the control of the constitutive 35S promoter in the *badc1 badc2* mutant. More than 10 independent lines were generated for each of *BADC1* and *BADC2* constructs into *badc1 badc2* (Supplemental Fig. S1). All transgenic lines demonstrated restored root growth to varying degrees, indicating the involvement of *BADC1* and *BADC2* in seedling development (Fig. 1, D and E). Because the *wri1* mutant (*wri1-1*) was recently shown to have a short-root phenotype during seedling establishment (Kong et al., 2017), we compared the growth of *badc1 badc2* and *wri1-1* under the same conditions and show

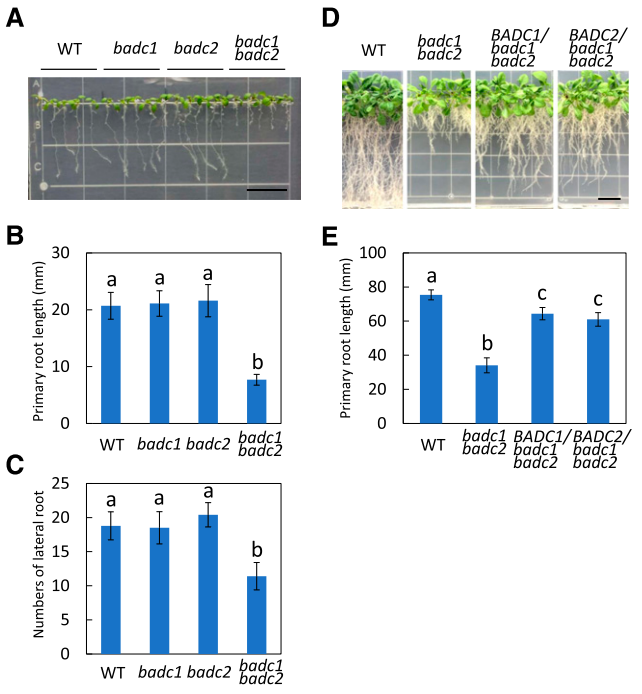

Figure 1. The *badc1 badc2* double mutant shows reduced primary root growth and fewer lateral roots than the wild type (WT). A, Nine-day-old wild-type, *badc1*, *badc2*, and *badc1 badc2* seedlings grown vertically on one-half strength MS media supplemented with 1% Suc. Bar = 13 mm. B, Primary root length measurement of each genotype in A. C, Lateral root numbers for each genotype in A. Values in B and C represent means ± SD from 10 individual plants for each genotype. D and E, Root growth (D) and primary root length (E) of 20-d-old wild-type, *badc1 badc2*, and representative transgenic *badc1 badc2* plants overexpressing *BADC1* or *BADC2* lines. Bar = 13 mm. Values in E are means ± SD from 10 individual plants for each indicated genotype. Lowercase letters above histogram bars indicate significant difference (Student's *t* test for all pairs of genotypes, $P < 0.01$). Data are representative of three independent repetitions.

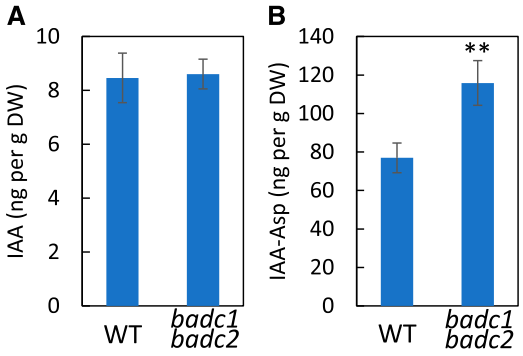

Figure 2. IAA-Asp content is significantly higher in the *badc1 badc2* double mutant than in the wild type (WT). A, Quantification of IAA in 7-d-old seedlings of wild type and *badc1 badc2*. B, Quantification of IAA-Asp in wild type and *badc1 badc2*. Values in this figure are means ± SD ($n = 4$) for each sample of 30 seedlings. Asterisks denote a statistically significant difference from the wild type (**$P < 0.01$; Student's *t* test). Data in this figure are representative of two independent repetitions.

that their phenotypes are visually indistinguishable (Supplemental Fig. S2).

Levels of Conjugated Auxin Were Elevated in *badc1 badc2* Plants Compared to Wild-Type Plants

In *wri1-1* the levels of IAA-Asp (a conjugated form of auxin thought to be destined for degradation [Ludwig-Müller, 2011]) were reported to be significantly elevated compared to the wild type (Kong et al., 2017). The similarity between the root phenotypes of *badc1 badc2* and *wri1-1* during seedling establishment prompted us to measure the levels of several growth hormones. As shown in Figure 2, IAA-Asp levels in 7-d-old seedlings showed a highly significant ~50% increase relative to levels found in the wild type. In contrast, the levels of free IAA and other plant hormones (i.e. abscisic acid, jasmonic acid, and salicylic acid) were not significantly different between *badc1 badc2* and the wild type (Fig. 2A; Supplemental Table S1).

WRI1 Interacts with AW Boxes from the Promoters of *BADC*s

That *badc1 badc2* mimics *wri1-1* in both its short-root phenotype and IAA-Asp content led us to hypothesize that *BADC*s are under transcriptional control of WRI1. Sequence analysis identified a canonical AW box consensus sequence within 200 bp upstream of the TIS in the promoters of all three *BADC* isoforms (Fig. 3A; Supplemental Table S2). To test whether WRI1 binds directly to these AW boxes, microscale thermophoresis (MST) assays were performed, in which a 28-bp double-stranded DNA fragment (Supplemental Table S2) containing each of the AW boxes from *BADC*s was titrated against purified WRI1 DNA binding domain (amino acids 58 to 240) fused with GFP (Supplemental Fig. S3). As shown in Figure 3, B and C, WRI1 exhibited low equilibrium dissociation constants (*K*), i.e. tight binding affinities for all three putative AW boxes, with *K* values between 0.27 and 5.24 nM, comparable to the affinity of WRI1 for the genuine AW box1 from the promoter of the WRI1 target gene *BCCP2* (0.65 nm; Maeo et al., 2009). Among the three *BADC* genes, WRI1 showed the highest affinity for the *BADC1* AW box at 0.27 ± 0.27 nM. The AW box from the *BCCP1* promoter was also tested, because although *BCCP1* contains an AW box (−60/−47 relative to the TIS), the gene was shown not to be regulated by WRI1 (Fukuda et al., 2013). Consistent with this, the *K* value for double-stranded DNA that includes the *BCCP1* AW box and WRI1 showed a *K* value ~37-fold higher than those for *BCCP2* and WRI1 (Supplemental Fig. S4). To test whether the consensus sequence [CnTnG](n)$_7$[CG] in *BADC* AW boxes is critical for WRI1 binding, three different mutant sequences were generated for each *BADC* AW box (Supplemental Table S2) and tested in MST. As shown in Supplemental Table S3, mutations in conserved nucleotides (m1 and m3) dramatically decreased their affinities to WRI1. Mutations in the seven nucleotides (m3) between also decreased their

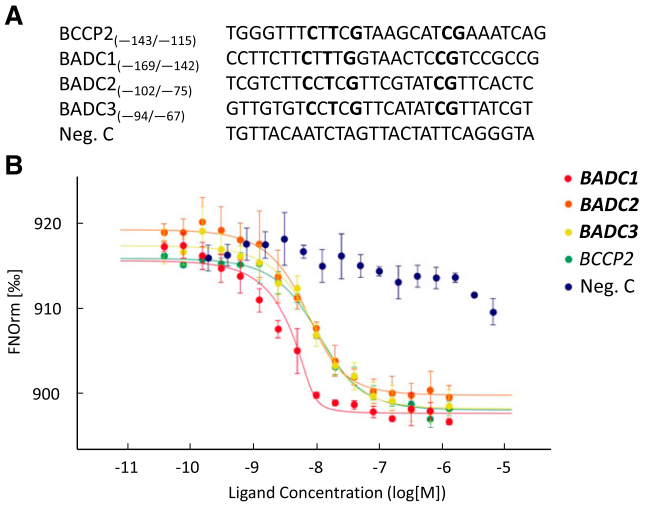

C

Target	Ligand	*Kd* (nM)
GFP-WRI1$_{58-240}$	*BCCP2*	0.65±0.39
	BADC1	0.27±0.27
	BADC2	2.73±0.72
	BADC3	5.24±2.59
	Neg.C	—

Figure 3. Purified WRI1 shows specific binding with AW boxes in the promoters of *BADC*s. In the thermophoresis experiment, a 28-bp oligonucleotide containing a putative AW box for each gene (A) was titrated against the purified WRI1 DNA binding domain (amino acids 58–240). Dissociation curves for each pair are shown (B) and fitted to the data for calculation of the *K* values (C). An AW box in the promoter of *BCCP2* was used as a positive control. A random sequence is used as a negative control (Neg. C). AW box consensus sequences are marked in bold. Data shown are the means ± SD, $n = 3$ independent repetitions.

affinity, but to a lesser degree because they are in a less conserved region (Supplemental Table S3).

BADC Expression and BADC1 Protein Levels Are Lower in Developing Siliques of *wri1-1* than in Those of the Wild Type

Gene expression quantification of *WRI1* and *BADC*s in different tissues (flower, silique, root, and mature leaf) showed tissue-specific expression patterns qualitatively similar to that of *WRI1* (Fig. 4A), i.e. high expression in siliques (developing seeds) and low expression in mature leaves. Because of the highest expression of *WRI1* and *BADC*s in developing seeds among analyzed tissues (Fig. 4A), siliques were selected for investigating the relationship between *WRI1* and *BADC*s. Gene expression of *BADCs* in developing siliques (7 d after flowering) of *wri1-1* were only 10% to 20% of that in the wild type (Fig. 4B). We next used a BADC1 antibody that showed high specificity toward BADC1 protein (Supplemental Fig. S5) to probe BADC1 levels in *wri1-1*. Consistent with the observed decreased expression of *BADC1* in *wri1-1* relative to the wild type, the level of BADC1 protein in *wri1-1* observed by immunoblotting was only 23% of that in the wild type (Fig. 4, C and D). Since relatively high gene expression of *WRI1* and *BADC*s was also observed in seedling roots (Fig. 4A), BADC1 protein level was quantified in seedling roots and was significantly lower in *wri1-1* seedling roots (12 d old) than in those of the wild type (Supplemental Fig. S6).

BADC Gene Expression and BADC1 Protein Levels Are Significantly Higher in Developing Siliques of *WRI1* Overexpressing Transgenic Plants than in Those of the Wild Type

To test whether overexpression of *WRI1* would increase gene expression of *BADCs* and the abundance of BADC1 polypeptide, we used two ethanol-inducible *WRI1* transgenic lines that were generated in our previous study (Zhai et al., 2017). Both lines demonstrated elevated WRI1 accumulation after induction with 2% (v/v) ethanol treatment (Zhai et al., 2017). As shown in Figure 5A, *BADC*, *WRI1*, and *BCCP2* expression in developing siliques of *WRI1* transgenic plants that were induced by irrigation with 2% (v/v) ethanol for 4 d was significantly higher than either the wild type or the corresponding *WRI1* transgenic plant lines that were not exposed to ethanol treatment (Fig. 5A). Consistent

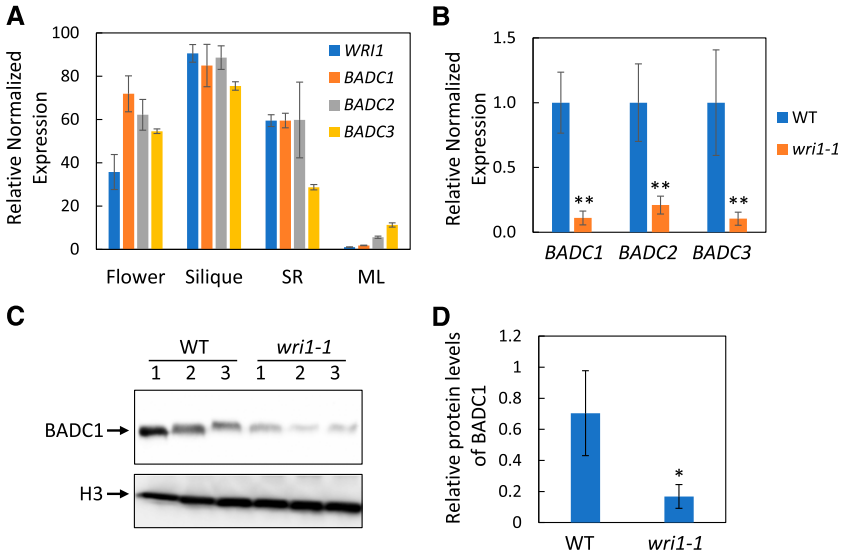

Figure 4. BADC expression and BADC1 protein level are significantly lower in wri1-1 developing siliques than in the wild type (WT). A, Tissue expression pattern of WRI1 and BADCs in flowers, siliques (7 d after flowering), seedling roots (SR; 10 d old) and mature leaves (ML). B, Reverse transcription quantitative PCR (RT-qPCR) results of BADC1, BADC2, and BADC3 expression in siliques (7 d after flowering) of wild-type and wri1-1 plants. For A and B, values are means ± SD from three independent experiments. Expression of each gene in the wild type was set to 1. For each experiment, total RNA was isolated from pooled siliques from wild-type and wri1-1 plants. *Fbox* (At5g15710) and *UBQ10* (At4g05320) were used as reference genes. Asterisks denote a statistically significant difference from the wild type (using mean crossing point deviation analysis computed by the relative expression [REST] software algorithm; **P < 0.01). C, BADC1 protein levels in siliques (7 d after flowering) of wild type or wri1-1 are shown by immunoblot with BADC1-specific antibody. Siliques were collected from three independent wild-type or wri1-1 mutant plants. Protein loading is shown by histone H3 in the same protein samples. D, Relative BADC1 protein levels in C quantified with GelAnalyzer2010 and normalized against corresponding protein levels of histone H3. The asterisk denotes a statistically significant difference from the wild type (*P < 0.05; Student's t test). Data in this figure are representative of three independent repetitions.

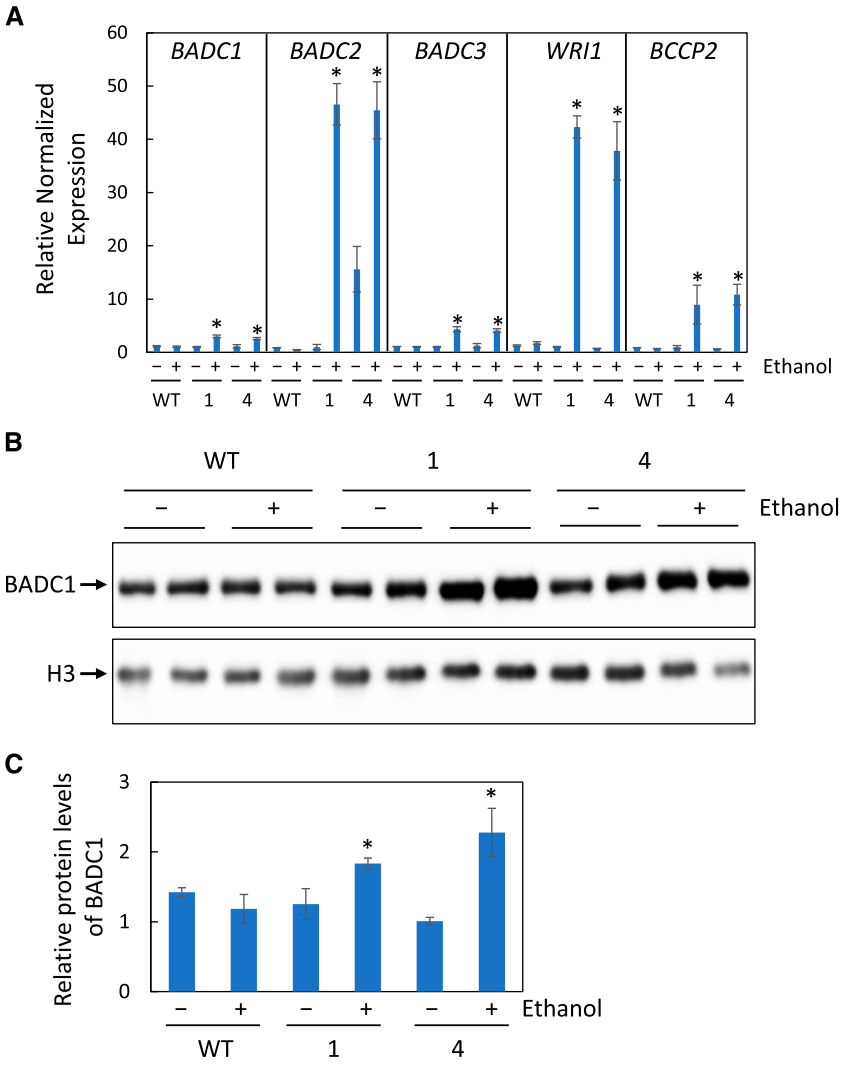

Figure 5. *BADC* expression and BADC1 protein levels are elevated in inducible *WRI1* transgenic plants. A, Relative gene expression of *BADC*s, *BCCP2*, and *WRI1* in siliques (7 d after flowering) of wild-type (WT) or two independent ethanol inducible *WRI1* transgenic lines (AlcA:*WRI1* line 1 and line 4) treated (+) or not treated (−) with 2% ethanol for 4 d. B, BADC1 protein levels. C, Relative BADC1 protein levels in B, quantified with GelAnalyzer2010 and normalized against corresponding protein levels of histone H3. Asterisks denote statistically significant difference from the wild type (*$P < 0.05$; Student's *t* test). Data in this figure are representative of three independent repetitions.

with the elevated expression of *BADC1*, BADC1 protein levels were also significantly higher upon *WRI1* overexpression (Fig. 5, B and C). To test whether global regulation of WRI1 on BADCs, gene expression, and protein levels were also quantified in the seedling roots of *WRI1* transgenics, as shown in Supplemental Figure S7, both gene expression and protein levels were higher in *WRI1* transgenics induced by ethanol treatment than either nonethanol treatment control or wild type (Supplemental Fig. S7).

Overexpression of BADC1 in *wri1-1* Partially Rescues the *wri1-1* Short-Root Phenotype

The data presented above support the hypothesis that the expression of *BADC* genes is under the control of WRI1 and that the short-root phenotype of *wri1-1* primarily results from a deficiency of *BADC1* and *BADC2*. To test this hypothesis, the coding sequence of *BADC1* was placed under the control of the 35S promoter and transformed into *wri1-1*. Fifteen of 17 independent transgenics demonstrated significantly longer primary root length than that of *wri1-1* when germinated and grown vertically on one-half strength MS medium plates for 16 d (Fig. 6, A and B). Immunoblotting showed BADC1 protein levels were significantly increased in the *BADC1/wri1-1* transgenics (Supplemental Fig. S8). To test whether the levels of IAA-Asp relate with the short-root phenotype of *wri1-1*, IAA contents were measured in 7-d-old seedlings of *BADC1/wri1-1*, *wri1-1*, and the wild type. The levels of IAA-Asp showed a significant decrease in *BADC1/wri1-1* relative to *wri1-1* (Fig. 6C), consistent with BADC1 playing a downstream role in WRI1-dependent root development.

DISCUSSION

In this work we establish that expression of *BADC1*, *BADC2*, and *BADC3* is under the transcriptional control of WRI1. Evidence to support this comes from: 1) identification of AW boxes within 200 bp upstream of

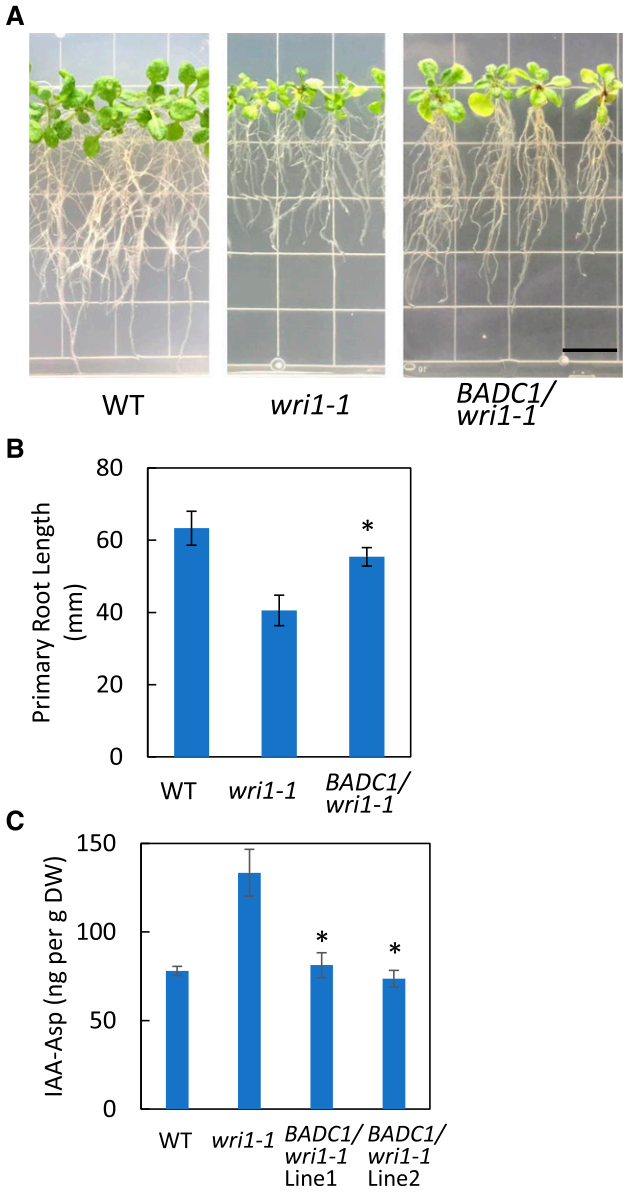

Figure 6. Overexpression of *BADC1* in *wri1-1* partially rescues *wri1-1* short-root phenotype. A and B, Root growth (A) and primary root length (B) measurement of 16-d-old wild-type (WT), *wri1-1*, and representative transgenic *wri1-1* overexpressing *BADC1* lines. Bar = 13 mm. Values in B are means ± SD from 10 individual plants for each indicated genotype. The asterisk denotes a statistically significant difference from the *wri1-1* mutant (*$P < 0.05$; Student's *t*- test). C, IAA-Asp was quantified in 7-d-old seedlings of wild-type, *wri1-1*, and *BADC1/wri1-1* transgenic lines 1 and 2. Asterisks denote statistically a significant difference from *wri1-1* (*$P < 0.05$; Student's *t* test). Data in this figure are representative of three independent repetitions.

the TIS; 2) MST measurement demonstrating tight binding, i.e. *K* values in the low nanomolar range between WRI1 and the AW boxes from all three *BADC* genes; 3) expression of each of the three *BADC* transcripts is reduced (by ~85%) in the *wri1-1* mutant; 4) protein levels of BADC1 are reduced similarly to reductions in the level of its transcript in the *wri1-1* mutant; and 5) both gene expression of *BADC*s and protein levels of BADC1 are increased upon overexpression of *WRI1*.

That WRI1, the master transcriptional activator of genes involved in FAS, simultaneously activates the transcription of *BADC*s, which have been shown to act as negative regulators of ACCase, might at first appear paradoxical. However, FAS is metabolically expensive in terms of both energy and reducing power, creating an imperative for tight metabolic control. For example, ACCase is generally acknowledged to be rate limiting with respect to FAS under tight genetic and biochemical control (Salie et al., 2016). When nonesterified FA levels in the cell were increased beyond demand by supplementation with Tween-esters, two phases of feedback inhibition were reported, one short term, the second longer term (Andre et al., 2012). Short-term inhibition occurs when the levels of oleoyl-ACP, the terminal product of the ACP track of FAS in the plastid, increase. Oleoyl-ACP inhibits ACCase by binding to it in a reversible manner (Andre et al., 2012). If, however, excess FA levels persist for 2 d or more, an irreversible phase of inhibition of ACCase is initiated that is primarily mediated by BADC1 and BADC3 (Keereetaweep et al., 2018). In this context, BADC subunits should not be regarded as a simple inhibitor, but rather as a conditional inhibitor of ACCase. Thus, coexpression of the ~20 genes that promote FAS, along with the three BADC subunits, makes biological sense. As WRI1 increases cellular metabolic demand by activating FAS, it concomitantly increases the capacity to downregulate ACCase, and thereby FAS, by increasing abundance of the conditionally inhibitory BADC subunits. Coregulation of FAS and the BADCs thus allows the cell to match synthetic capacity with its regulatory capacity. The biochemical regulation of ACCase described herein is complementary to the transcriptional regulation of FAS we recently reported, in which levels of the WRI1 polypeptide are tightly coupled to the availability of cellular carbon in the form of sugars. When the carbon/energy status of the cell decreases, the SnRK1 carbon-sensing kinase becomes activated and phosphorylates WRI1, leading to its selective proteasomal degradation, thereby reducing activation of *FAS* genes (Zhai et al., 2017). Conversely, when carbon/energy abundance increases, levels of the SnRK1 kinase inhibitor trehalose 6-phosphatase increase, reducing WRI1 phosphorylation/degradation, thereby increasing the amount of WRI1 available to activate transcription of *FAS* genes (Zhai et al., 2018).

In this study we also observed that the *badc1 badc2* double mutant exhibits reduced primary root growth, a phenotype that resembles that of the *wri1-1* mutant (Kong et al., 2017), which in combination with our finding that WRI1 controls *BADC* transcription led us to ask whether the short-root phenotype characteristic of both *wri1-1* and *badc1 badc2* mutants results from a deficit of BADC. If correct, overexpression of *BADC* in *wri1-1* would mitigate the *wri1-1* short-root phenotype.

This view is supported by the observation that overexpression of *BADC1* in *wri1-1* partially rescued the short-root phenotype in a manner similar to its overexpression in the *badc1 badc2* mutant background (and as overexpression of *BADC2* had in the *badc1 badc2* mutant background). Consistent with this, the elevated levels of IAA-Asp observed in *wri1-1* were restored to wild-type levels in *BADC1/wri1-1*. Taken together, these observations suggest that deficiency of BADC levels, resulting either directly via mutation of *badc* genes, or indirectly through the mutation of their upstream transcriptional activator, *wri1*, result in a short-root phenotype via a mechanism yet to be determined. Further work will be required to identify details of the mechanism, which is likely related to increased levels of conjugated IAA that were observed for both *wri1-1* and *badc1 badc2* mutants.

Taken together, we show that all three *BADC* genes are direct target genes of WRI1 and can play a role in root development. The observation that WRI1 upregulates not only genes contributing to FAS, but also BADCs, which are conditional regulators of FAS, identifies an additional layer of regulation with respect to FAS.

MATERIALS AND METHODS

Plant Materials and Growth Conditions

Wild-type Arabidopsis (*Arabidopsis thaliana* ecotype Columbia-0) and *wri1-1* (CS69538), *badc1* (Salk 000817C), *badc2* (Salk 021108C), and *badc3* (CS2103834) were used in this study. The double mutant *badc1 badc2* was generated as described previously by Keereetaweep et al. (2018). For growth on plates, seeds were surface sterilized with 70% (v/v) ethanol, followed by 30% (v/v) bleach containing 0.01% Tween20, and rinsed three times with sterile water. Seeds were stratified for 3 d at 4°C in the dark and germinated on one-half strength MS medium supplemented with 1% (w/v) Suc plates in an incubator with a light/dark cycle of 18h/6h at 23°C, photosynthetic photon flux density of 250 μmol m^{-2} s^{-1}, and 75% relative humidity.

Genetic Constructs

Coding sequences of *BADC1* and *BADC2* were amplified by PCR from cDNAs using the primers listed in Supplemental Table S4. The PCR products were then cloned into the Invitrogen GATEWAY™ pDONR/Zeo vector (Thermo Fisher Scientific) using the BP reaction and subcloned (LR reaction) into the plant GATEWAY binary vector pGWB414 (Nakagawa et al., 2007). *BADC1*/pGWB414 and *BADC2*/pGWB414 were introduced into *badc1 badc2* double mutants by *Agrobacterium tumefaciens* (AgL0)-mediated transformation. For rescuing the short-root phenotype of *wri1-1*, *BADC1*/pGWB414 was transformed into *wri1-1*.

Quantification of IAA, IAA-Asp in *badc1 badc2* Double Mutant Seedlings

Seven-day-old Arabidopsis wild-type and *badc1 badc2* seedlings grown vertically on one-half strength MS medium supplemented with 1% (w/v) Suc were harvested (20–30 seedlings per replicate, ~100 mg fresh weight) and frozen in liquid nitrogen. Frozen samples were sent to the Proteomics & Mass Spectrometry Facility at the Donald Danforth Plant Science Center for acidic hormone analysis, where frozen plant material was extracted twice with ice-cold acetonitrile/methanol (1:1 v/v) using a bead beater and resulting samples were dried with the use of a speedvac. Samples were reconstituted in 30% MeOH and separated via HPLC using a Waters Acquity UPLC BEH C18 1.0 × 100 mm, 1.7 μm column kept at 50°C with a flow rate of 15 μL/min coupled to an AB Sciex 6500 QTrap mass spectrometer operated in multiple reaction monitoring mode employing polarity switching for simultaneous detection of positive and negative ions. Data analysis was completed using MultiQuant 3.0.2 (AB Sciex) with unlabeled compound peak areas normalized to their respective labeled internal standard peak areas. Labeled standards for IAA and IAA-Asp were obtained from Sigma-Aldrich. Calibration curves were linear ($r > 0.99$) within the ranges provided above and applying 1/x weighting.

RNA Isolation and RT-qPCR

To quantify gene expression in mutants and transgenic plants, total RNA was isolated using the RNeasy Plant Mini Kit (Qiaqen). cDNA was prepared using SuperScript IV VILO Master Mix with ezDNase Enzyme (Invitrogen). RT-qPCR reactions were set up with SsoAdvanced Universal SYBR Green Supermix (Bio-Rad) and gene-specific primers (primer sequences are listed in Supplemental Table S4) and performed with the CFX96 qPCR Detection System (Bio-Rad). Statistical analysis of RT-qPCR data were carried out with REST2009.

Expression and Purification of Recombinant GFP-WRI1$_{58–240}$

The DNA sequence of full-length WRI1 fused with GFP on its N terminus (*GFP-WRI1*) was amplified from an OWD5 (Oleosin+WRI1+DAGT1) vector previously described in Zhai et al. (2017). *GFP-WRI1* then was inserted into pet28b between *XhoI* and *NcoI* by in-fusion cloning. Full-length *WRI1* in the resulting *GFP-WRI1*/pet28b was replaced with the DNA sequence corresponding to the WRI1 DNA binding domain (WRI1$_{58–240}$) between *XhoI* and *BsrGI* (Kong et al., 2017). The primer pairs used in building this construct are listed in Supplemental Table S4. Recombinant GFP-WRI1$_{58–240}$ was expressed in *Escherichia coli* BL21(DE3). Protein purification was performed as reported by Zhai et al. (2017).

MST

Thermophoretic assays were conducted using a Monolith NT.115 apparatus (NanoTemperTechnologies). For determining *K* values, 8 nM of GFP-WRI1$_{58–240}$ was incubated with a serial dilution of the ligand (double-stranded DNA) from 1.25 μM to 38.81 pM. Samples of ~10 μL were loaded into capillaries and inserted into the MST instrument loading tray (Monolith NT.115). The thermophoresis experiments were carried out using 40% MST power and 80% LED power at 25°C.

Antibody and Immunoblotting

Anti-BADC1 and antihistone H3 antibodies were used in this study. Anti-BADC1 antibodies were requested from Dr. Jay Thelen (Salie et al., 2016). Histone H3 polyclonal antibodies were purchased from Agrisera (catalog no. AS10710). A total of 50 mg of siliques (7 d after flowering) of wild-type and *wri1-1* mutant plants were ground in liquid nitrogen and then mixed with 200 mL of preheated protein extraction buffer (8 M urea, 2% SDS, 0.1 M dithiothreitol, 20% glycerol, 0.1 M Tris-HCl, pH 6.8, and 0.004% Bromophenol Blue). Samples were centrifuged at 17,000 × *g* before transferring the supernatant to a new microcentrifuge tube and then loading into SDS-PAGE. Twenty μL of supernatant was loaded and resolved in SDS-PAGE and transferred onto polyvinylidene difluoride membrane for immunoblot analysis. Primary antibodies of anti-BADC1 were used at a 1:3,000 dilution, and the anti-H3 antibodies were used at a 1:5,000 dilution. Immunoblots of targeted proteins were visualized using horseradish peroxidase-conjugated secondary antibodies (catalog no. AP187P, Millipore) with SuperSignal West Femto Maximum Sensitivity Substrate (Catalog No. 34095, ThermoFisher). Immunoblot signals were detected and digitalized with Image Quant LAS4000 and quantified with GelAnalyzer2010a.

Accession Numbers

Sequence data from this article can be found in The Arabidopsis Information Resource under the following accession numbers: AT3G54320 (*WRI1*), AT3G56130 (*BADC1*), AT1G52670 (*BADC2*), AT3G15690 (*BADC3*), AT5G16390 (*BCCP1*), AT5G15530 (*BCCP2*), AT5G15710 (*Fbox*), and AT4G05320 (*UBQ10*).

Supplemental Data

The following supplemental materials are available.

Supplemental Figure S1. *BADC1* expression in transgenic *badc1 badc2* double mutants overexpressing *BADC1* lines.

Supplemental Figure S2. *badc1 badc2* shows a short-root phenotype similar to that of *wri1-1*.

Supplemental Figure S3. Purified recombinant GFP-WRI1$_{58-240}$.

Supplemental Figure S4. Putative AW boxes show varied binding affinity with WRI1.

Supplemental Figure S5. The BADC1 antibody used in this study specifically recognizes BADC1.

Supplemental Figure S6. BADC1 protein levels are lower in the roots of seedlings of *wri1-1* than in the wild type.

Supplemental Figure S7. Both *BADC1* expression and protein levels are elevated in the roots of *WRI1*-inducible expression transgenic plants.

Supplemental Figure S8. BADC1 protein levels in the *BADC1/wri1-1* transgenic lines.

Supplemental Table S1. Quantification of plant hormones in *badc1 badc2* double mutant seedlings.

Supplemental Table S2. Nucleotide sequences of AW boxes in the thermophoretic experiment.

Supplemental Table S3. Binding affinity of *BADC* AW boxes with and without mutations to WRI1 were quantified as equilibrium dissociation constants (*K*) using MST.

Supplemental Table S4. Oligonucleotide sequences of primers used in this study.

ACKNOWLEDGMENTS

We thank Dr. Jay Thelen (University of Missouri) for the gift of the BADC1 antibody.

Received May 14, 2019; accepted June 7, 2019; published June 17, 2019.

LITERATURE CITED

Andre C, Haslam RP, Shanklin J (2012) Feedback regulation of plastidic acetyl-CoA carboxylase by 18:1-acyl carrier protein in *Brassica napus*. Proc Natl Acad Sci USA **109:** 10107–10112

Baud S, Mendoza MS, To A, Harscoët E, Lepiniec L, Dubreucq B (2007) WRINKLED1 specifies the regulatory action of LEAFY COTYLEDON2 towards fatty acid metabolism during seed maturation in Arabidopsis. Plant J **50:** 825–838

Braybrook SA, Stone SL, Park S, Bui AQ, Le BH, Fischer RL, Goldberg RB, Harada JJ (2006) Genes directly regulated by LEAFY COTYLEDON2 provide insight into the control of embryo maturation and somatic embryogenesis. Proc Natl Acad Sci USA **103:** 3468–3473

Focks N, Benning C (1998) *wrinkled1*: A novel, low-seed-oil mutant of Arabidopsis with a deficiency in the seed-specific regulation of carbohydrate metabolism. Plant Physiol **118:** 91–101

Fukuda N, Ikawa Y, Aoyagi T, Kozaki A (2013) Expression of the genes coding for plastidic acetyl-CoA carboxylase subunits is regulated by a location-sensitive transcription factor binding site. Plant Mol Biol **82:** 473–483

Grimberg Å, Carlsson AS, Marttila S, Bhalerao R, Hofvander P (2015) Transcriptional transitions in *Nicotiana benthamiana* leaves upon induction of oil synthesis by WRINKLED1 homologs from diverse species and tissues. BMC Plant Biol **15:** 192

Kagaya Y, Okuda R, Ban A, Toyoshima R, Tsutsumida K, Usui H, Yamamoto A, Hattori T (2005) Indirect ABA-dependent regulation of seed storage protein genes by FUSCA3 transcription factor in *Arabidopsis*. Plant Cell Physiol **46:** 300–311

Keereetaweep J, Liu H, Zhai Z, Shanklin J (2018) Biotin attachment domain-containing proteins irreversibly inhibit acetyl CoA carboxylase. Plant Physiol **177:** 208–215

Kong Q, Ma W, Yang H, Ma G, Mantyla JJ, Benning C (2017) The Arabidopsis WRINKLED1 transcription factor affects auxin homeostasis in roots. J Exp Bot **68:** 4627–4634

Li Q, Shao J, Tang S, Shen Q, Wang T, Chen W, Hong Y (2015) Wrinkled1 accelerates flowering and regulates lipid homeostasis between oil accumulation and membrane lipid anabolism in *Brassica napus*. Front Plant Sci **6:** 1015

Li-Beisson Y, Shorrosh B, Beisson F, Andersson MX, Arondel V, Bates PD, Baud S, Bird D, DeBono A, Durrett TP (2013) Acyl-lipid metabolism. The Arabidopsis Book **8:** e0161, doi:10.1199/tab.0133

Lotan T, Ohto M, Yee KM, West MA, Lo R, Kwong RW, Yamagishi K, Fischer RL, Goldberg RB, Harada JJ (1998) Arabidopsis LEAFY COTYLEDON1 is sufficient to induce embryo development in vegetative cells. Cell **93:** 1195–1205

Ludwig-Müller J (2011) Auxin conjugates: Their role for plant development and in the evolution of land plants. J Exp Bot **62:** 1757–1773

Maeo K, Tokuda T, Ayame A, Mitsui N, Kawai T, Tsukagoshi H, Ishiguro S, Nakamura K (2009) An AP2-type transcription factor, WRINKLED1, of *Arabidopsis thaliana* binds to the AW-box sequence conserved among proximal upstream regions of genes involved in fatty acid synthesis. Plant J **60:** 476–487

Mu J, Tan H, Zheng Q, Fu F, Liang Y, Zhang J, Yang X, Wang T, Chong K, Wang X-J, et al (2008) *LEAFY COTYLEDON1* is a key regulator of fatty acid biosynthesis in Arabidopsis. Plant Physiol **148:** 1042–1054

Nakagawa T, Suzuki T, Murata S, Nakamura S, Hino T, Maeo K, Tabata R, Kawai T, Tanaka K, Niwa Y, et al (2007) Improved gateway binary vectors: High-performance vectors for creation of fusion constructs in transgenic analysis of plants. Biosci Biotechnol Biochem **71:** 2095–2100

Ohlrogge J, Browse J (1995) Lipid biosynthesis. Plant Cell **7:** 957–970

Olinares PDB, Ponnala L, van Wijk KJ (2010) Megadalton complexes in the chloroplast stroma of *Arabidopsis thaliana* characterized by size exclusion chromatography, mass spectrometry, and hierarchical clustering. Mol Cell Proteomics **9:** 1594–1615

Parcy F, Valon C, Kohara A, Miséra S, Giraudat J (1997) The ABSCISIC ACID-INSENSITIVE3, FUSCA3, and LEAFY COTYLEDON1 loci act in concert to control multiple aspects of Arabidopsis seed development. Plant Cell **9:** 1265–1277

Rawsthorne S (2002) Carbon flux and fatty acid synthesis in plants. Prog Lipid Res **41:** 182–196

Ruuska SA, Girke T, Benning C, Ohlrogge JB (2002) Contrapuntal networks of gene expression during Arabidopsis seed filling. Plant Cell **14:** 1191–1206

Salie MJ, Zhang N, Lancikova V, Xu D, Thelen JJ (2016) A family of negative regulators targets the committed step of de novo fatty acid biosynthesis. Plant Cell **28:** 2312-2325

Santos Mendoza M, Dubreucq B, Miquel M, Caboche M, Lepiniec L (2005) LEAFY COTYLEDON 2 activation is sufficient to trigger the accumulation of oil and seed specific mRNAs in Arabidopsis leaves. FEBS Lett **579:** 4666–4670

To A, Valon C, Savino G, Guilleminot J, Devic M, Giraudat J, Parcy F (2006) A network of local and redundant gene regulation governs Arabidopsis seed maturation. Plant Cell **18:** 1642–1651

Zhai Z, Liu H, Shanklin J (2017) Phosphorylation of WRINKLED1 by KIN10 results in its proteasomal degradation, providing a link between energy homeostasis and lipid biosynthesis. Plant Cell **29:** 871–889

Zhai Z, Keereetaweep J, Liu H, Feil R, Lunn JE, Shanklin J (2018) Trehalose 6-phosphate positively regulates fatty acid biosynthesis by stabilizing WRINKLED1. Plant Cell **30:** 2616–2627